EXERGY ANALYSIS ON TURBOCHARGER RADIAL TURBINE WITH HEAT TRANSFER

SM. Lim - A. Dahikild - M. Mihaescu*

Competence Center for Gas Exchange (CCGEx),
KTH Royal Institute of Technology, Stockholm, Sweden
*Corresponding author, email: smlim@kth.se

ABSTRACT

Inconsistent results about heat transfer effects on performance and poor understanding of the aerothermodynamics loss mechanisms related to heat transfer in turbocharger turbine motivated this study. This study aimed to investigate the sensitivity of performance to heat loss and to quantify loss mechanisms associated with heat transfer in a turbine by using exergy analysis. A hybrid simulation methodology, i.e. Detached Eddy Simulation (DES) was used to compute the three-dimensional flow field of a turbine operating under hot gas stand continuous flow condition. Principal findings of this study were 1) Pressure ratio is less sensitive to heat loss as compared to turbine power, 2) Turbine power drop due to heat loss is relatively insignificant as compared to the exergy lost by heat transport and exergy destroyed by thermal irreversibilities, and 3) Assuming the most ideal isentropic gas expansion, more than 80% of the inflow exergy is unutilized in the investigated turbine system.

KEYWORDS

EXERGY, TURBINE, TURBOCHARGER, HEAT TRANSFER, EFFICIENCY, DES

Latin letters

T	[K]	Temperature
P	[$\mathrm{ML^{-1}T^{-2}}$]	Pressure
s	[$\mathrm{L^2T^{-2}K^{-1}}$]	Specific static entropy
I	[$\mathrm{L^2T^{-2}K^{-1}}$]	Irreversibilities
Q	[$\mathrm{ML^2T^{-2}}$]	Heat flow
W	[$\mathrm{ML^2T^{-2}}$]	Work
m	[M]	Mass
n	[$\mathrm{T^{-1}}$]	Rotational speed
h	[$\mathrm{L^2T^{-2}}$]	Specific enthalpy
c_p	[$\mathrm{L^2T^{-2}K^{-1}}$]	Specific heat
Be	[-]	Bejan number
e_f	[$\mathrm{L^2T^{-2}}$]	Specific flow exergy
v	[$\mathrm{L^3M^{-1}}$]	Specific volume

Greek letters

π	[-]	Pressure ratio
η	[-]	Efficiency/Utilization
Φ	[$\mathrm{L^2T^{-2}}$]	Mechanical dissipation function
μ	[$\mathrm{ML^{-1}T^{-1}}$]	Dynamic viscosity
λ	[$\mathrm{MLT^{-3}K^{-1}}$]	Thermal conductivity
κ	[-]	Specific heat ratio

Subscripts

t	Total quantity
T	Turbine
o	Dead state quantity
w	Wall
$Isen$, $Adia$	Isentropic, Adiabatic
ex	Exergetic
in, out	Inflow, outflow

Superscripts

$\dot{()}$	[$\mathrm{T^{-1}}$]	Time derivative
$\overline{()}$		Statistical average

INTRODUCTION

Stricter environmental policies for automotive vehicles in terms of fuel economy and tail-end pollutant emissions have been implemented worldwide in the past decades. In order to fulfill the legislation requirements, automotive manufacturers constantly seek for innovative ideas to develop even more fuel-efficient and low-emission Internal Combustion Engines (ICE). One of the important technologies employed is the *engine downsizing*, where the associated unavoidable performance loss with the smaller engine size is compensated by the usage of a turbocharger unit to maintain the same power output of the engine.

In turbocharging, the otherwise wasted exhaust gases from the engine combustion are used to drive a turbine. A compressor, which is connected to the turbine via a common shaft is then used to increase the density of the intake air for a more efficient combustion process. Heat transfer effects are significant in the turbochargers. For example, the turbine can lose heat to the external ambient via radiation and to the compressor side through internal conduction. Despite of the presence of heat transfer, turbocharger's performance is derived from enthalpy rise across the compressor stage under adiabatic conditions. Thus, the performance of the turbine (e.g. turbine power and efficiency) is estimated from the work input to the compressor (under adiabatic assumption), by considering the energy balance on the common rotating shaft. This has driven the research towards focusing on how the heat transfer from the hot turbine side impacts the performance of the compressor (e.g. Rautenberg et al., 1984; Bohn et al., 2005). Parameters that are negatively affect compressor's efficiency were identified (e.g. Shaaban and Seume, 2006). Efforts were also made towards building simplified heat transfer models to correct for heat transfer effects and to predict more realistic compressor performance parameters (e.g. Romagnoli and Martinez-Botas, 2012; Baines et al., 2010). As for the turbine side, a large number of studies are focusing on reducing errors associated with predicting turbine outlet temperature (e.g. Burke et al., 2015).

Although there are some studies about how the heat transfer affects the performance of the turbine, the conclusions are contradictory. For example, Shaaban and Seume (2012) conducted an experimental study on a turbocharger operating under continuous flow conditions on a gas stand. The turbine was fed with cold (T_{in}= 305 K) and hot (T_{in}= 973 K) gases, which represents adiabatic and diabatic conditions, respectively. The study showed that under hot gas conditions at low speed operating points, the turbine efficiency is about 20% lower (equivalent to 55% turbine power reduction), as compared with cold gas conditions. Furthermore, Shaaban and Seume (2012) also found that the efficiency of an insulated turbine operating under hot gas stand conditions is almost similar to that of a turbine operated with cold gases, and thus concluded that heat losses can significantly reduce the turbine power. The findings corresponded well to the thermodynamic theory about negative effects of heat loss on turbocharger turbine performance.

On the other hand, Serrano et al. (2007) showed that turbine efficiency is about 4% higher under hot gas conditions (T_{in}= 875 K), as compared with cold gas conditions (T_{in}= 525 K). The percentage of efficiency improvement is within the measurement uncertainty range and the authors attributed this to the improvement of mechanical efficiency due to lower lubricant oil viscosity in hot gas conditions. In another work, Sirakov and Casey (2013) studied experimentally how different heat transfer levels affect the performance of the turbocharger under gas stand steady flow conditions. The amount of heat transfer in the turbocharger was varied by cooling the center housing between the turbine and the compressor with water and by changing the turbine inlet temperature. Their measurements showed that the pressure ratio is insensitive to the amount of heat transfer and the authors concluded that heat transfer hardly

affects the aerothermodynamics of the turbocharger. On the other hand, the apparent efficiency of the compressor and turbine was found to be highly sensitive to heat transfer, particularly at low speed and low mass flow operating conditions. Sirakov and Casey (2013) attributed this to the misinterpretation of temperature rise in the compressor due to heat transfer as additional work required to compress the air. Since turbine power and efficiency are derived from compressor power and efficiency through power balance assumption, the turbine appears to have better efficiency than the real condition. There is a shift of efficiency from the compressor to the turbine and the effects of heat transfer is simply a misinterpretation of the energy flow in the turbocharger. In a numerical study by using Large Eddy Simulations (LES) with wall function, Hellström and Fuchs (2010) found that the difference in turbine shaft power is less than 1% between adiabatic and diabatic scenarios under engine-like pulsating flow conditions.

From the discussions above, it can be seen that researchers have not reached consensus about heat transfer effects on the performance of turbocharger turbine. Most literature deal with direct comparisons of turbine performance between adiabatic and non-adiabatic scenarios by employing total energy balance analysis, which is based on the first law of thermodynamics. Little effort is done to identify and to quantify the mechanisms of heat transfer associated aerothermodynamics losses in turbocharger turbine.

The objectives of this study were to investigate the sensitivity of performance to heat loss and to quantify aerothermodynamics loss mechanisms associated with heat transfer in a turbine by using Detached Eddy Simulation (DES). The scope of the study was limited to the fluid domain of the turbine, operating under hot gas stand continuous flow conditions. Sensitivity of the turbine performance parameters (i.e. turbine pressure ratio and power) was investigated under adiabatic and several non-adiabatic scenarios. Furthermore, exergy analysis, which is based on both the first and the second law of thermodynamics was employed to identify and to quantify the mechanicms of heat transfer related aerothermodynamics losses. The effectiveness of the turbine system to utilize the available resources was also investigated with exergy analysis.

METHODOLOGY & CASE SETUP

Numerical Methods

A hybrid technique, i.e. Detached Eddy Simulation (DES) was used for all simulations in this study. Two-equation SST (Shear Stress Transport) $k-\omega$ (Menter, 1994) was used as the underlying Reynolds Averaged Navier-Stokes (RANS) turbulence model in the near-wall region, while the core-flow region was solved by using Large Eddy Simulation (LES) with Smagorinsky subgrid-scale (SGS). Improved Delayed DES (IDDES) formulation proposed by Shur et al. (2008) was adopted to minimize the Logarithmic Layer Mismatch (LLM) issue at the interface between the RANS and the LES regions. Hybrid methodology was adopted to reduce near-wall grid resolution, and hence lowering the computational cost, as compared with wall-resolved LES (Gourdain et al., 2014).

In this study, Star-CCM+, a fully compressible density-based CFD solver with finite volume formulation developed by CD-Adapco was used for mesh generation and numerical simulations. Mass, momentum and energy conservation equations were solved in transient manner. The working medium in the turbine was assumed to be air, which behaves according to the ideal gas law. The temperature dependent behaviour of dynamic viscosity and thermal conductivity were modelled with Sutherland's Law. The specific heat of air was modelled by using a temperature dependent fourth degree polynomial function. Implicit time stepping with second order temporal discretization was employed. As for the spatial discretization, implicit hybrid

bounded-central differential (BCD) scheme was used. The rotation of the turbine wheel was modeled by using Sliding mesh technique, i.e. the turbine wheel is rotated physically at every time-step. Prior to transient simulations, steady-state RANS based on SST $k-\omega$ turbulence model with mixing plane stationary-rotating interface was performed. The steady-state RANS flow field was then used to initialize the flow fields of DES simulations. The transient simulations were then run for a total of fourty five turbine wheel revolutions. The results of the first five revolutions were discarded to eliminate any initial transient effects. The results of the remaining fourty revolutions were sampled at every ten time-steps to derive statistically converged data with about 0.3% standard deviation.

Computational Model

The object of this study was a vaneless and wastegated turbocharger radial turbine mounted on a 2.0-liter, four-cylinder spark-ignition (SI) passenger vehicle engine. The turbine wheel has twelve blades, with inlet to outlet diameter ratio of about 1.2. Fig. 1 shows the computational domain used in this study. The computational domain represents the hot gas stand experimental setup, which was used to measure the steady performance map of the turbine. It consists of an inlet pipe, a scroll, a rotating turbine wheel, outlet pipe 1 and 2. In the gas stand experiment, measurements were done in the plane z_1, which is located in the outlet pipe 1. The outlet pipe 2 was included in the computational domain to ensure that the flow field at plane z_1 is being computed, rather than directly imposed by the outlet boundary conditions. In order to account for windage loss and tip leakage flow, the gaps between the rotating turbine wheel and the backplate as well as the tip clearance between the rotating turbine wheel and the shroud wall, were also considered. Note that the wastegate bypass channel was not included in the computational domain because the wastegate was closed in the hot gas stand experiment.

The computational domain was discretized by using polyhedral control volume. Regions far upstream from the scroll (i.e. inlet pipe) and downstream from the turbine wheel (i.e. outlet pipe 2) consist of hexahedral cells, which were extruded from the polyhedral cells up to the inlet and outlet boundaries. The grid densities in the turbine wheel and the outlet pipe 1 are approximately double as compared with the scroll to capture the blade curvature and to resolve the complex turbulence flow field in those regions. Prism layers with a 1.1 stretching factor were employed to capture the flow and temperature gradients at the near-wall regions in the wall normal direction.

The model used in this study has about nine million cells, with 0.7 mm average cell edge length. Twelve prism layers were used and this resulted in y^+ of 2 and 0.2 in maximum and average values, respectively. The computational grid was validated and verified by a grid sensitivity study, where the sensitivity of grid size to global performance parameters (i.e. pressure ratio and turbine torque), mean and fluctuating quantities of flow variables, heat transfer rate and energy spectra were assessed (Lim, 2006).

Boundary Conditions

The boundary conditions imposed correspond to the point of maximum efficiency on a low speed line of turbine performance map measured in the hot gas stand. This operating point was chosen because literature observations show that heat transfer has larger impact on the turbine performance at low speed lines (e.g. Shaaban and Seume, 2012; Burke et al., 2015). At the inlet boundary plane, uniform mass flow rate $\dot{m}_{in}$ =0.058 kg/s and total temperature $T_{t_{in}}$=1173 K were imposed. The gas was assumed to enter the computational domain in the

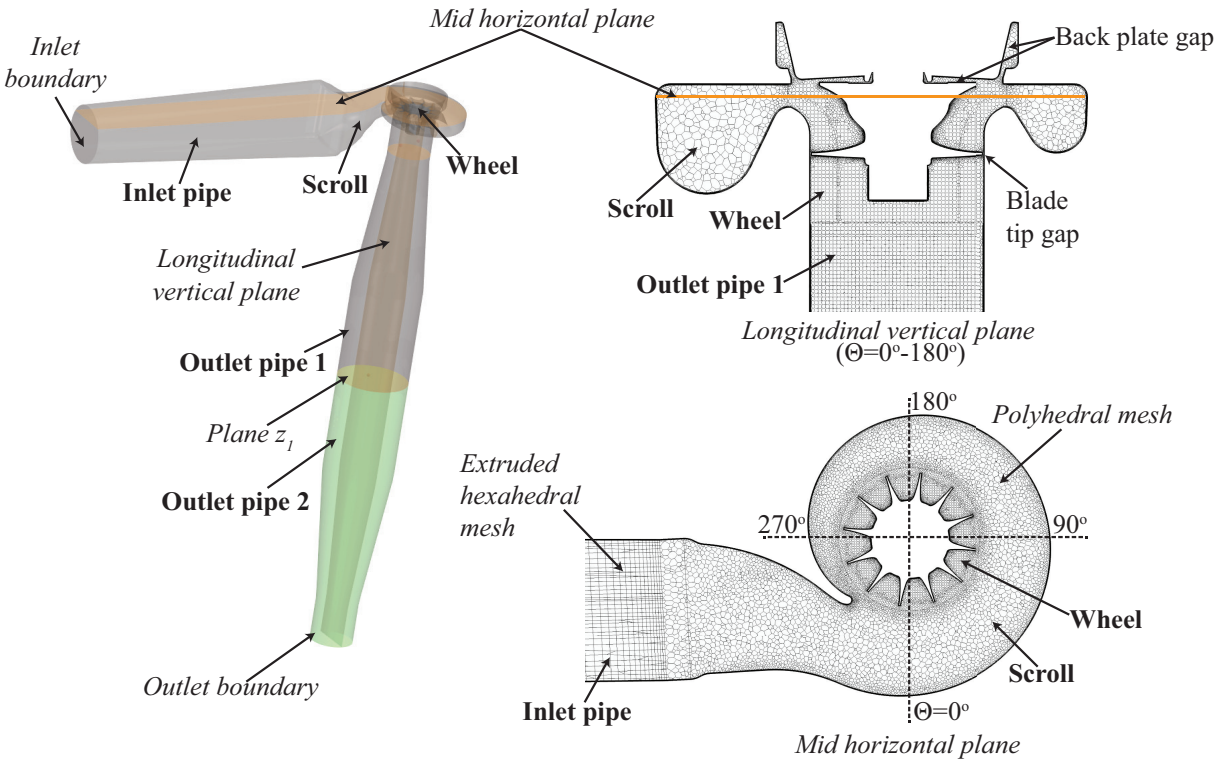

Figure 1: **Computational domain and grid. Experimental measurements were done at inlet boundary plane and plane z_1 in the hot gas stand.**

direction perpendicular to the inlet boundary plane, with 5% turbulent intensity estimated from fully developed turbulent pipe flow. Constant atmospheric pressure was considered at the outlet boundary plane. The turbine wheel was rotated at constant speed n=84533 rpm, with time-step of 1.97162x10^{-6}s. The selected time-step corresponds to three degrees of turbine wheel rotation per time-step, and it's ability to reproduce turbine transient behavior (e.g. blade passing event) at reasonable computational cost has been verified (Lim, 2006). Smooth wall and no-slip conditions were employed to all walls.

Since no information about heat transfer conditions were available from the gas stand measurements, the turbine heat loss was modeled by assuming a constant wall temperature T_w= 1002 K on all walls. The value was estimated from experimentally measurued average turbine scroll's wall temperature published by Romagnoli and Martinez-Botas (2012). Despite its simplicity, the assumption of constant wall temperature should not hinder the purpose of investigating the sensitivity of turbine performance to total heat loss, and demonstrating the application of exergy analysis to quantify heat transfer related losses. Additional cases with adiabatic wall and T_w= 830 K and 487 K were also setup to mimic different heat transfer level. Note that the mass flow average of gas static temperatures after expansion were computed to be about 1064 K, 997 K and 854 K at plane z_1 for T_w= 1002 K, 830 K and 487 K, respectively. As the gas static temperatures after expansion is higher than the applied wall temperatures, the turbine is operating under cooled expansion, i.e. heat transfer from the gas to the wall.

Computation Resources

All simulations were performed on the *Beskow* supercomputer at KTH, which is a Cray XC40 system with 53632 compute cores in total (1676 node with 32 cores per each). In this study, 320 cores were used for each test case. With the computational setup described before, the computational time per test case was about seven hours.

HEAT TRANSFER SENSITIVITY

Fig. 2a shows the sensitivity of pressure ratio π and turbine power $\dot{W}_T$ to the total heat loss $\dot{Q}_{total}$. π was defined as the ratio of the absolute total pressure at the inlet boundary plane to the absolute static pressure at the plane z_1. Mass flow average was used to evaluate the flow variables over the planes. As for $\dot{W}_T$, it was calculated as the dot product of turbine torque and rotational speed vectors. The turbine torque was computed as the sum of the cross product of the position and the total force (pressure and shear components) vectors acting on the rotating blades. $\dot{Q}_{total}$ was computed by integrating the heat flux over the wall surfaces up to outlet pipe 1. Overline bar denotes statistical average. The data on the vertical axis is normalized by the performances computed with adiabatic wall, i.e. a value of one means there is no deviation of performance from the adiabatic scenario. At the horizontal axis, $\dot{Q}_{total}$ is normalized by the corresponding $\dot{W}_T$ as an indication of the relative magnitude between heat and work transfer.

From Fig. 2a, it can be observed that π remains unaffected by heat loss until the total heat loss is about as large as the turbine power ($\overline{\dot{Q}_{total}}/\overline{\dot{W}_T} \approx 1$). When heat loss is significantly larger than the work transfer ($1 < \overline{\dot{Q}_{total}}/\overline{\dot{W}_T} \leq 5.5$), an approximately linear decrease in π with a mild slope is observed. On the othe hand, $\dot{W}_T$ is observed to be relatively more sensitive to heat loss, as compared to π. A linear drop in $\dot{W}_T$ with a steeper slope is observed whenever there is a heat loss. This indicates that if direct torque measurements are not possible in an experiment, there is a risk of making wrong conclusion about heat transfer effects on turbine power by just comparing the measured turbine pressure ratio under adiabatic and diabatic scenarios.

The lost in power for cases with heat loss appears to be related to the diminished expansion of the gas as it is cooled ideally. A reversible turbine working isochorically with heat loss (see Fig. 2b) can be worked out to give a power of 91% of the isentropic (adiabatic and reversible) turbine for the given pressure ratio. The lost heat is then about 3 times the turbine power.

EXERGY ANALYSIS

The specific flow exergy of a flowing gas is a state variable defined by

$$e_f = h_t(T_t, P_t) - h_o - T_o \cdot [s(T_t, P_t) - s_o] \,, \tag{1}$$

where h_t is the specific total enthalpy and s is the specific static entropy. The definition requires also specification of the so called dead state (subscript o), at which the gas is at equilibrium with its surroundings. Here, we chose T_o= 298.15 K and P_o= 101325 Pa.

The value of the flow exergy of a uniform gas flow, $\dot{m} \cdot e_f$, represents the maximum amount of shaft work that can be extracted in an open system which let the fluid continuously passing through, interact with the surroundings until the fluid element is at equilibrium with the surroundings. If the gas comes to in equilibrium with the surroundings, no more shaft power can be extracted from the gas flow. An analysis of the flow exergy budget of a turbine system can be used to quantify the heat transfer related losses by using the computed three dimensional flow field data.

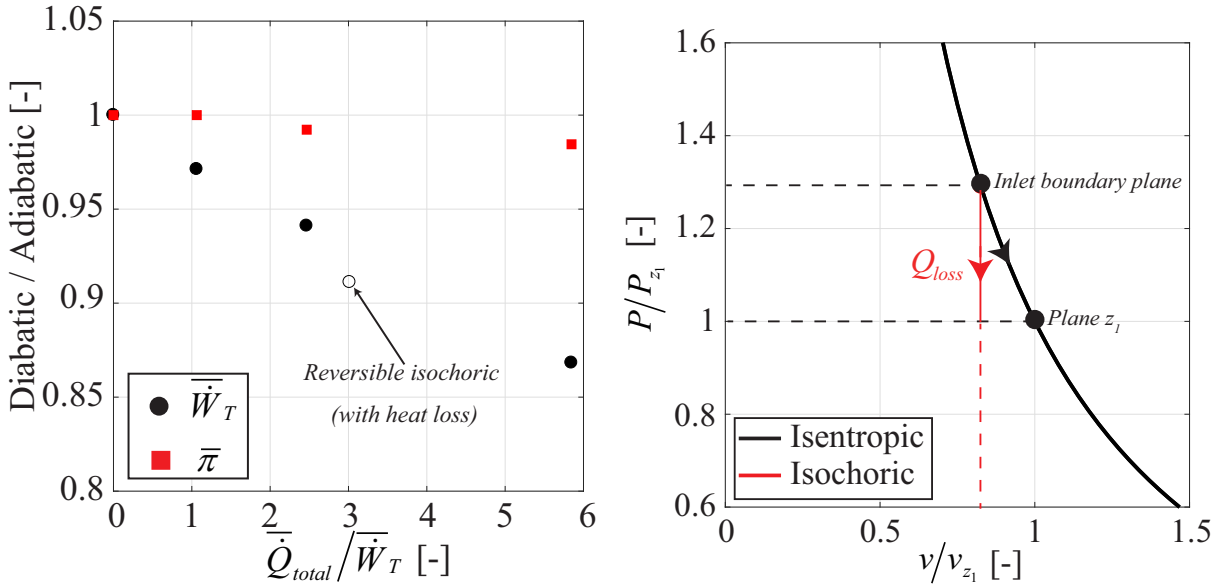

(a) **Global performances** (b) **Reversible isochoric process**

Figure 2: **(a) Sensitivity of turbine global performances to heat loss. (b) Simplified reversible isochoric process with heat loss. Axes are normalized with data at plane z_1.**

Since the investigated operating point corresponds to the maximum efficiency point, the turbine can be approximated as a steady flow device. Lim (2006) has confirmed the validity of this assumption by showing that although transient simulations were performed, the average time dependent term was found to be insignificant. Therefore, the flow exergy budget for a steady flow system applies as in Eq. 2, by combining the energy balance to the entropy balance times T_o.

$$\dot{m} \cdot \Delta e_f = \dot{m} \cdot (e_{f_{in}} - e_{f_{out}}) = \underbrace{-\sum_j \left(1 - T_o/T_w\right) \cdot \dot{Q}_j}_{A} + \underbrace{\dot{W}_T}_{B} + \underbrace{T_o \cdot \dot{I}_{total}}_{C} \; . \tag{2}$$

where $\dot{Q}_j$ is the heat flow rate through the system boundary in j^{th}-component (e.g. inlet pipe, scroll, and etc) and it is negative for heat loss. $\dot{W}_T$ is positive here because work is done by the system. $\dot{I}_{total}$ is the total irreversibilities (or entropy generation) within the system and it is always equal or greater than zero (see Eq. 3). Note that unlike the energy balance, flow exergy is not conserved, due to irreversibilities within the system, which can be expressed as

$$\begin{aligned} \dot{I}_{total} &= \dot{I}_{viscous} + \dot{I}_{thermal} \\ &= \iiint_V \left[\frac{\mu}{T} \cdot \Phi\right] dx\, dy\, dz + \iiint_V \left[\frac{\lambda}{T^2} \cdot (\nabla T)^2\right] dx\, dy\, dz \; . \end{aligned} \tag{3}$$

μ and λ are the effective (sum of the molecular and turbulent contributions) dynamic viscosity and the thermal conductivity of the gas, respectively. Φ is the mechanical dissipation function, as defined below in cartesian tensor form.

$$\begin{aligned}\Phi &= \tau_{ij} \cdot \frac{\partial u_i}{\partial x_j} \\ &= 2 \cdot S_{ij} \cdot S_{ij} - \frac{2}{3} \cdot S_{kk} \cdot S_{kk} \ .\end{aligned} \tag{4}$$

where τ_{ij} and $\frac{\partial u_i}{\partial x_j}$ are the shear stress and velocity gradient tensors, respectively. S_{ij} is the strain rate tensor, as defined below.

$$S_{ij} = \frac{1}{2} \cdot \left(\frac{\partial u_i}{\partial x_j} + \frac{\partial u_j}{\partial x_i} \right) . \tag{5}$$

From Eq. 2, it can be seen that the net change of flow exergy in the turbine system is due to three mechanisms, i.e. exergy lost by heat transport (term A), the harvested exergy by extracting turbine work (term B) and the exergy destroyed by irreversibilities generated within the turbine system (term C). Exergy lost by heat transport can also be considered as exergy destruction in the turbine system, since the associated heat flow out from the system boundary cannot be further utilized for useful work.

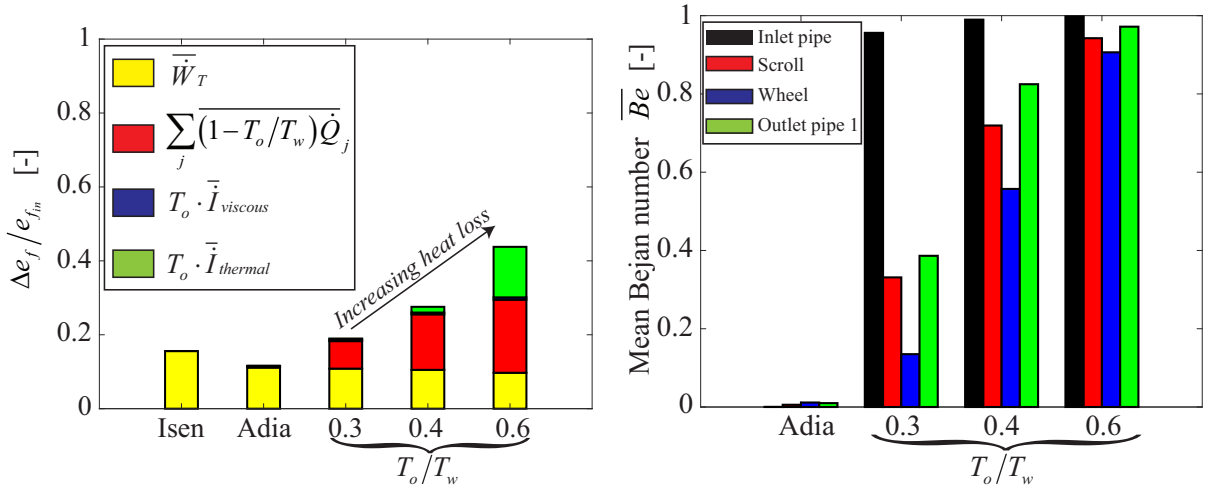

(a) **Overall exergy budget** (b) **Mean Bejan number**

Figure 3: **Exergy analysis (a) Overall exergy budget (b) Mean Bejan number. Overline denotes statistical mean value. Isen and Adia are the abbreviations for Isentropic and Adiabatic, respectively.**

An overall exergy budget for the turbine system, as shown in Fig. 3a, is plotted to investigate the effect of heat loss to each mechanism (represented by different colors in the stacked bar). The data on the vertical axis is normalized by the inflow exergy, i.e. the value of one is the maximum exergy that can be extracted for useful work from the system (not restricted to turbine only). Note that T_o/T_w is used to represent the diabatic scenarios. From Fig. 3a, it can be seen that the heat loss increases the exergy lost by heat transport, as expected. Thermal irreversibilities also increase due to heat transfer as a result of larger temperature gradient. On the other hand, viscous irreversibilities remain relatively small although the heat loss increases. As for the turbine power, it decreases linearly with increasing heat loss following the discussions in the previous section.

From Fig. 3a, it can also be observed that with heat loss, although most of the exergy is destroyed via heat transport and thermal irreversibility mechanisms, the drop of turbine power is only a small percentage of the total inflow exergy. An exergetic utilization η_{ex} can be defined as in Eq. 6 to indicate how efficient the turbine system utilizes the inflow exergy.

$$\eta_{ex} = \frac{\dot{W}_T}{\dot{m} \cdot e_{f_{in}}} \tag{6}$$

It is clear from Fig. 3a that even in the desirable adiabatic scenario, η_{ex} is only about 11%, and this indicates underutilization of resources. In the adiabatic scenario, the unutilized flow exergy is discharged as high temperature gas out from the turbine system. With heat loss, part of the exergy is destroyed via irreversibilities and heat transport in the turbine system, while the remaining unutilized exergy is discharged out with lower exhaust gas temperature.

The discussions above show that there is a great potential to improve exergy utilization in the system. However, the theoretical maximum turbine power is the isentropic expansion power, which is governed by the inlet total temperature and the pressure ratio (see Eq. 7). Assuming that an isentropic expansion can be achieved, η_{ex} is still about 16%, as can be seen from Fig. 3a. Note that the isentropic efficiency η_{Isen} as defined in Eq. 8 for the adiabatic turbine (no η_{Isen} can be defined for cases with heat transfer) is about 71%. This indicates that high η_{Isen} does not necessary indicate effective utilization of resources.

$$\dot{W}_{T_{Isen}} = \dot{m} \cdot c_p \cdot T_{t_{in}} \left(1 - \pi^{-(\kappa-1)/\kappa}\right) \tag{7}$$

$$\eta_{Isen} = \frac{\dot{W}_{T_{Adia}}}{\dot{W}_{T_{Isen}}} \tag{8}$$

The relative importance of viscous and thermal irreversibilities can be quantified by using Bejan number Be (Bejan, 1995), as defined below.

$$Be = \frac{1}{1 + \dot{I}_{viscous}/\dot{I}_{thermal}} \tag{9}$$

From Eq. 9, it is obvious that Be ranges from zero to one. Larger value indicates thermal irreversibilities dominant and lower value means viscous irreversibilities dominant. From Fig. 3b, it can be seen that in general, Be increases with increasing heat loss for all components (e.g. inlet pipe, scroll, and etc.), as expected. However, the rate of increment of Be for each component is different. For example, Be of inlet pipe jumps from $\sim$0 to $\sim$1 when there is heat transfer and it remains approximately constant with increasing heat loss. Downstream components like the scroll, the turbine wheel and the outlet pipe 1 show more gradual increment of Be with increasing heat loss. This implies that the more upstream the component, the more sensitive the component subjects to thermal irreversibilities. This is because the more upstream the component, the larger the temperature difference between the gas and the wall. Beside temperature difference between the gas and the wall, the amount of heat loss also depends on the surface area to volume ratio. Therefore, it is important to insulate the upstream component (due to large temperature difference between the wall and gas) and downstream component which has large surface to volume area (i.e. scroll) if one would like to reduce the thermal irreversibilities in the turbine system.

With three dimensional flow field data, one can visualize the spatial distribution of flow exergy and Be, as shown in Fig. 4. Here, we use the mid horizontal plane cutting through the scroll as an example. Since no work is extracted in the scroll, the change of flow exergy represents the combine effects of exergy lost by irreversibilities and heat transport. It can be observed that flow exergy (left) reduces spatially when heat loss increases, especially at near-wall region. Be contour (right) explains that the reduction of flow exergy is due to the increase of thermal irreversibilities as a result of larger gradients in temperature (especially at near-wall region) field when heat transfer level increases.

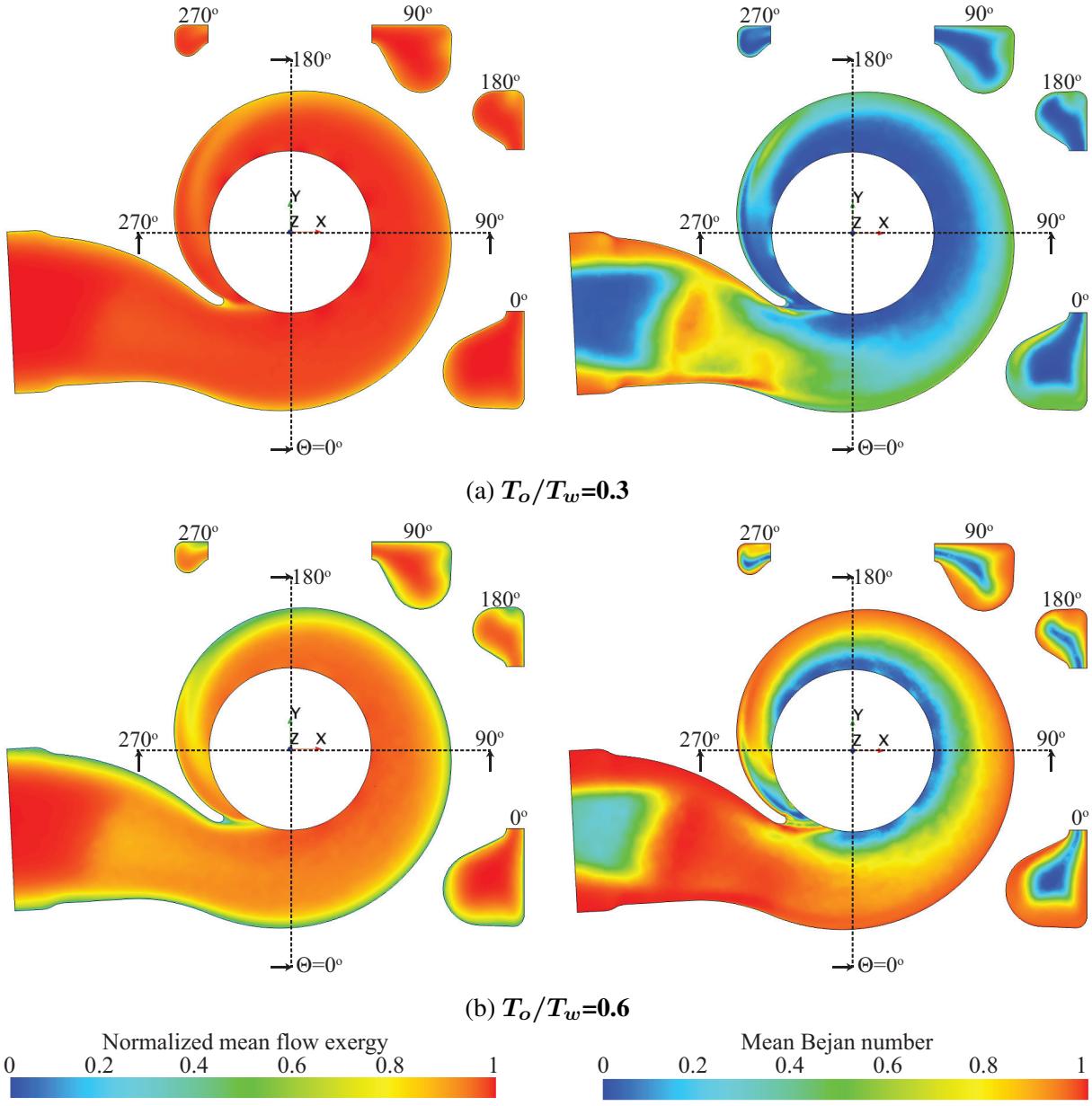

Figure 4: **Comparisons of mean flow exergy (left) and mean Bejan number (right) contours in the scroll at mid horizontal plane for (a) T_o/T_w=0.3 (b) T_o/T_w=0.6. Mean flow exergy is normalized by mass flow average of mean flow exergy at the inlet boundary plane.**

CONCLUSIONS

In this study, we showed that turbine power is less sensitive to heat loss, as compared to pressure ratio. Exergy analysis showed that turbine power drop due to heat loss is relatively small, as compared to the increase of exergy lost by thermal irreversibilities and heat transport. Possibly, if operating points at higher pressure ratio were considered, such that the obtained power due to expansion of the gas is essential, heat losses accompanied by less gas expansion might have a larger effect on the turbine power.

Furthermore, at the investigated operating point, an exergy analysis showed that the utilization of available exergy associated by the turbine system is as low as 16% even under idealized isentropic expansion. This indicates that there is potential to improve better resource utilization. However, factors such as economical benefit, design complexity, and etc. should be considered also if one would like to replace the turbine with other exergetically more efficient devices.

Constant wall temperature was imposed as thermal boundary condition to model the turbine heat loss in this study. More realistic thermal boundary condition with non-uniform wall temperature could be obtained by performing Conjugate Heat Transfer (CHT) in the future. Nevertheless, this study showed that exergy analysis could be used to quantify the heat transfer related aerothermodynamics losses in a turbine with heat transfer.

Although this study chose a turbine working under hot gas stand continuous flow conditions as an example of exergy analysis, exergy analysis can be extended to turbine operating under engine-like pulsating flow conditions (Lim, 2006). This enables us to investigate the effectiveness of exhaust gas utilization and to quantify the heat transfer associated aerothermodynamics losses in realistic engine conditions.

ACKNOWLEDGEMENTS

This study was performed within the framework of the Competence Center for Gas Exchange (CCGEx) at KTH. The authors would like to acknowledge the supports and contributions from Scania, Volvo GTT, Volvo Cars, Swedish Energy Agency and Borg Warner. The Swedish National Infrastructure for Computing via Parallel Computing Center (PDC) at KTH is also acknowledged for providing the computational resources.

REFERENCES

Baines, N., Wygant, K. D., and Dris, A. (2010). The analysis of heat transfer in automotive turbochargers. *Journal of Engineering for Gas Turbines and Power*, 132(4):042301.

Bejan, A. (1995). *Entropy generation minimization: the method of thermodynamic optimization of finite-size systems and finite-time processes*. CRC press.

Bohn, D., Heuer, T., and Kusterer, K. (2005). Conjugate flow and heat transfer investigation of a turbo charger. *Journal of engineering for gas turbines and power*, 127(3):663–669.

Burke, R., Vagg, C., Chalet, D., and Chesse, P. (2015). Heat transfer in turbocharger turbines under steady, pulsating and transient conditions. *International Journal of Heat and Fluid Flow*, 52:185–197.

Gourdain, N., Sicot, F., Duchaine, F., and Gicquel, L. (2014). Large eddy simulation of flows in industrial compressors: a path from 2015 to 2035. *Philosophical Transactions of the Royal Society of London A: Mathematical, Physical and Engineering Sciences*, 372(2022).

Hellström, F. and Fuchs, L. (2010). Assessment of heat transfer effects on the performance of a radial turbine using large eddy simulation. In *9th International Conference on Turbochargers and Turbocharging; Westminster, London; United Kingdom; 19 May 2010 through 20 May 2010*, pages 281–291.

Lim, S. M. (2006). Flow and heat transfer in a turbocharger radial turbine. Technical report, KTH Royal Institute of Technology, Sweden. ISBN: 978-91-7729-238-8. http://urn.kb.se/resolve?urn=urn:nbn:se:kth:diva-197916.

Menter, F. R. (1994). Two-equation eddy-viscosity turbulence models for engineering applications. *AIAA journal*, 32(8):1598–1605.

Rautenberg, M., Malobabic, M., and Mobarak, A. (1984). Influence of heat transfer between turbine and compressor on the performance of small turbochargers. In *IN: 1983 Tokyo International Gas Turbine Congress, Tokyo, Japan, October 23-29, 1983, Proceedings. Volume 2 (A85-41776 20-07). Tokyo, Gas Turbine Society of Japan, 1984, p. 567-574.*, volume 2, pages 567–574.

Romagnoli, A. and Martinez-Botas, R. (2012). Heat transfer analysis in a turbocharger turbine: An experimental and computational evaluation. *Applied Thermal Engineering*, 38:58 – 77.

Serrano, J., Guardiola, C., Dolz, V., Tiseira, A., and Cervello, C. (2007). Experimental study of the turbine inlet gas temperature influence on turbocharger performance. Technical report, SAE Technical Paper.

Shaaban, S. and Seume, J. (2006). Analysis of turbocharger non-adiabatic performance. In *Eighth International Conference on Turbochargers and Turbocharging*.

Shaaban, S. and Seume, J. (2012). Impact of turbocharger non-adiabatic operation on engine volumetric efficiency and turbo lag. *International Journal of Rotating Machinery*, 2012.

Shur, M. L., Spalart, P. R., Strelets, M. K., and Travin, A. K. (2008). A hybrid RANS-LES approach with delayed-DES and wall-modelled LES capabilities. *International Journal of Heat and Fluid Flow*, 29(6):1638 – 1649.

Sirakov, B. and Casey, M. (2013). Evaluation of heat transfer effects on turbocharger performance. *Journal of Turbomachinery*, 135(2):021011.